Available online at www.sciencedirect.com

SciVerse ScienceDirect

Ceramics International 39 (2013) 1631–1637

CERAMICS INTERNATIONAL

www.elsevier.com/locate/ceramint

Study of the nanoparticle/microparticle powder systems by dry dispersion

I. Lorite*, J.J. Romero, J.F. Fernandez

Instituto de Cerámica y Vidrio, ICV-CSIC, 29049 Madrid, Spain

Received 7 June 2012; received in revised form 1 August 2012; accepted 1 August 2012
Available online 15 August 2012

Abstract

The study of a nanoparticle/microparticle powder systems by dispersion of different type of nanoparticles over microparticles, as support or substrate, has been afforded by a soft mechanical and solvent-less procedure and its effect on the electrostatic charge was studied. The dispersion degree can be evaluated by using diffuse reflectance measurements due to the non-linear change of the reflectance as a function of the nanoparticles amount in the powder composite. The maximum slope variation of the non-linear curve revealed the point where the nanodispersion attained the highest efficiency. The interaction between the OH groups of the dissimilar surfaces provides the anchoring mechanism of the nanoparticles onto the microparticles and the net charge compensation. Furthermore, the dispersed and anchored nanoparticles provide a roughness increasing of the microparticles surface that is responsible for a formation of nanoparticle/microparticle composite powders in which tribo-charge maximized due to the enhancement of composite packaging.

Keywords: B. Nanocomposites; Nanoparticles; Oxidess; Coating

1. Introduction

The materials at the nano-scale usually present unusual properties which are different to their bulk counterpart. Nanotechnology implies the use of the properties arising in materials having almost one of the dimensions below 100 nm. In this area of knowledge the oxide nanoparticles have attracted large scientific interest because their properties are the base for the development of new products in different fields as cosmetic, catalyst, polymer based nanocomposites, ceramics, etc. The oxide nanoparticles have a strong tendency to agglomerate due to electrostatic and Van der Waals forces [1], which is a drawback as it could change their outstanding properties and therefore limit their applications. To overcome the mentioned drawbacks, highly dispersed nanoparticles are required, making the dispersion of nanoparticles a subject of many research efforts. Most of the processes have in common the use of high energy tools in liquid media that usually are combined with surfactants to prevent the re-agglomeration upon drying.

In order to effectively take advantage of the nanoparticles properties new concepts are needed. Composites formed by hierarchically ordered nanoparticles and microparticles allow the use of microparticles as carriers or vector to hold the nanoparticles and eventually promoted nanoparticle dispersion. Those kind of composites nanoparticles/microparticles can find application in electronic [2], photocatalysis [3] or biological markers [4].

The dispersion and anchoring of nanoparticles over a specific support can provide new or enhanced properties as a function of the agglomeration state, as, for example, new Co_3O_4 [5] surface magnetism, changes in the optical properties due to the NiO/substrate interaction [6], higher rates in catalysis applications [7]. Usually, the nanoparticles are anchored on different functionalized surfaces, dithiols capped gold substrates [8] or aminoalkylalkoxysilanes on silica substrates [9,10]. In general the presence of chemical molecules, typically surfactants change the surface properties of the nanoparticles and make difficult their use for specific applications. Solvent-free processes are being

*Corresponding author.
E-mail address: ilorite@icv.csic.es (I. Lorite).

0272-8842/$ - see front matter © 2012 Elsevier Ltd and Techna Group S.r.l All rights reserved.
http://dx.doi.org/10.1016/j.ceramint.2012.08.005

nowadays investigated in an attempt to avoid covering the nanoparticle surface that can cause undesirable effects, as well as avoiding the solvent cost. Simple methods as electrostatic spraying charge, based on the principle of electrostatic interaction, have been proposed [11].

On the way of searching for a solvent-free dispersion procedure applicable to oxide nanoparticles, the dry dispersion of fine particles on larger substrate by soft mechanical impacts has been proposed by Hersey [12]. This process is designed for microparticles as the morphology remain unalterated. In this kind of process, the electrostatic charge can be a problem as it takes great relevance for dry powders due to the impacts between particles and the equipment walls [13]. In order to gain advantage of the electrostatic charge in oxide powders for the above mentioned processes, a understanding of both the net and the tribo-charge has to be established. Electrostatic charge on metal oxides has been associated to differences in the nature of the surface OH groups [14]. Moreover, the nature of the surface OH groups changes with the size of the oxide particle and this change is more pronounced for submicronic particles, as we demonstrated recently [15]. The surface OH groups can act as a link between two dissimilar particles to provide particle–particle interactions or proximity effects. These effects have been described as electrochemical reactions taking place at room temperature between solid oxide particles. This interaction produces a surface magnetic like behavior on Co_3O_4 nanoparticles dispersed over different oxide microparticles by solvent-free processes [16].

The present work affords the design of powder composites formed by dispersions of Co_3O_4 and NiO nanoparticles over microparticles. The powders were chosen by the properties variation produced by the dry dispersion of the nanoparticles over the substrates. Moreover, the study of the electrostatic properties of these composites gave a tool to control the size of agglomerates of the composites, important for the nanoparticles properties.

2. Experimental procedure

Two different micrometric powders were used as microparticles substrates: α-Al_2O_3,with a purity $>99{,}5\%$ and average particle size of $\sim 6\,\mu m$ (Vicar S.A., Manises, Spain) that consisted of platelet shaped particles; and ZnO with a purity $>99.5\%$ (Aldrich) and particle size of $0.5\,\mu m$, having different morphologies from nearly spherical particles to needle type ones. On the other hand, Co_3O_4 and NiO were used as nanoparticles (both from Aldrich). Co_3O_4 has a purity $>99.9\%$ and average particle size of $\sim 30\,nm$. The Co_3O_4 nanoparticles form large agglomerates with $>5\,\mu m$ in diameter. NiO nanoparticles have a purity of 99.9% with particle size $\sim 20\,nm$ and form agglomerates larger than $10\,\mu m$.

Hierarchically ordered composites having different contents of nanoparticles in wt% were prepared. They will be named hereafter as AlCo*X*, AlNi*X*, ZnCo*X* and ZnNi*X* where the first element refers to the oxide microparticle (acting as substrate), the second one to the oxide nanoparticle and *X* is the proportion of nanoparticles in wt%. The composites were prepared following a previously described dry nanodispersion method [17]. The dry dispersion process consisted on mechanical milling of the adequate mixtures of nanoparticles and microparticles using a turbula-type mixer at room temperature. The powders were introduced in a $60\,cm^3$ nylon container and mixed during 10 min at 500 rpm. The process was assisted by the addition of Al_2O_3 balls (1 mm in diameter). The same process of mechanical milling was carried out for each of the as received powders, both nanoparticles and microparticles, separately, in order to ensure that any changes in the particles structure were not introduced by the nanodispersion process. Before the dry mixing process, all powders were separately dried at 100 °C for 4 h.

Measurement of the net and tribo charge of pure powders and composites were obtained using a double Faraday cup [18]. This device was a set of two stainless steel cylindrical cages of different diameter which were insulated from each other by a Teflon® plate. These two cages were concentric to each other and connected to an electrometer (Keithley 6517A, Cleveland, Ohio, USA). The inner container surrounds the charged object, who induces an equal and opposite charge on the inner wall of the cylinder. This charge is drawn from the capacitor of the electrometer to which the pail was connected. The outer cage was grounded to define a reference point and eliminate external signals. To carry out the charge characterization, the powders were dried at 100 °C for 4 h and handled with a grounded stainless steel scoop in order to remove the charge produced by friction. The experimental setup included an electronic balance to determine the powder weight in each measurement, in order to normalize the charge measured by the powder mass. The process was repeated 10 times for each powder by using new samples of about 2 g each. Two different experiments were done: in one of them the intrinsic or net charge was obtained once the powder is directly dropped in the inner cage; on the other one, the tribo charge of the powder was measured passing the powders along a glass cylinder of 50 cm in length inclined at 45°. At the end of the glass cylinder the powder reach the Faraday cage. The as recieved powders possess different charge and polarity, as shown in Table 1, that justify their use in the present study.

Field Emission Scanning Electron Microscopy (FESEM, Hitachi S-4700, Tokyo, Japan) was used to study the samples morphology by acquiring secondary electron images. To obtain an estimation of the nanoparticle dispersion efficiency in the powder composites, UV–vis spectra for the different proportions were acquired with a Pelkin Elmer series 9000 electrometer equipped with an integrating sphere.

The average agglomeration diameter of the powder composites after the tribo-charge measurements was determined by image analysis on micrographs obtained by Light Reflected

Table 1
Net electrostatic charge and Tribo-charge of the starting powders.

	Al_2O_3	ZnO	Co_3O_4	NiO
Net Charge (nC/g)	0.12 ± 0.16	-0.44 ± 0.12	0.22 ± 0.08	0.08 ± 0.03
Tribo-charge (nC/g)	2.48 ± 0.35	1.68 ± 0.33	0.71 ± 0.19	-0.54 ± 0.24

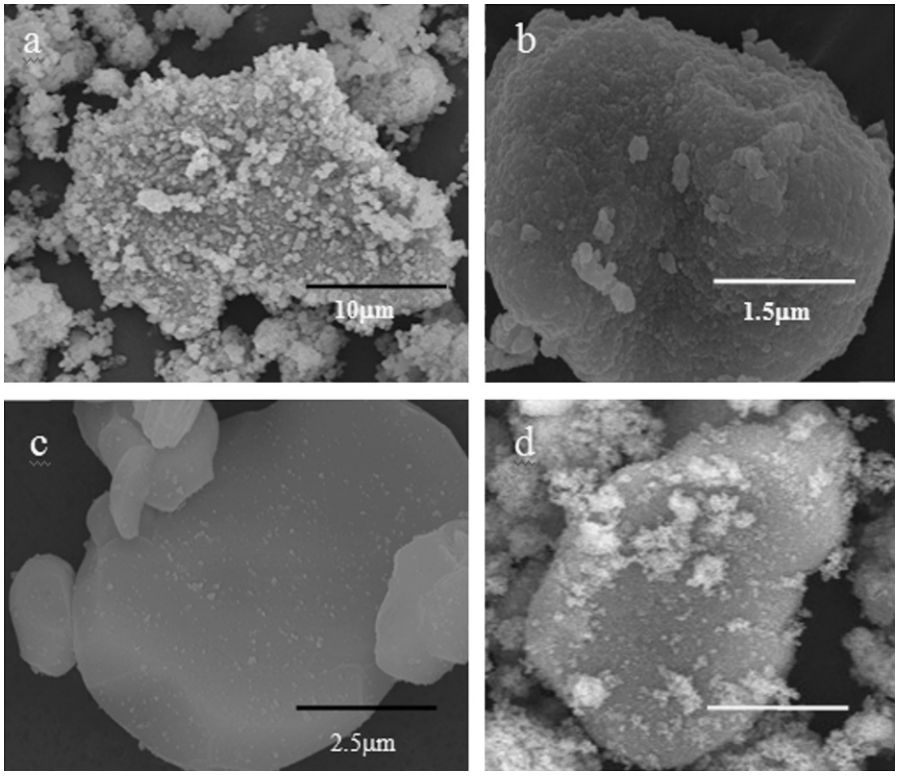

Fig. 1. Scanning electron microscopy for different metal oxide mixtures nanoparticles of (a) Co_3O_4; (b) NiO; (c) AlCo1 and (d) AlCo10.

Optical Microscopy. The number of agglomerates measured was >200 to obtain an accurate value.

Infrared characterization, ATR-IR, (Spectrum 100 TF-IR, PerkinElmer, Massachusetts, USA) was used to study hydroxylation of the particles surface.

3. Results and discussion

Fig. 1 shows the Field Emission Scanning Electronic microscopies of starting Co_3O_4, NiO nanoparticles and powder composites AlCo1, AlCo10. The platelet morphology of alumina microparticles is well suited to observe the nanoparticles dispersion on their surface. The morphology of the supporting microparticles remained unaltered after the dispersion because of the low energy employed during the dry mixing procedure. As it can be seen in the powder composites having low amount of Co_3O_4 nanoparticles (AlCo1), Fig. 1c, the nanoparticles are dispersed and nearly individually located at the alumina surface. Co_3O_4 agglomerates comparable to the as received agglomerates were not found after an intensive search. As the amount of nanoparticles increased in the powder composites (AlCo10, Fig. 1d), both dispersed, nearly individual nanoparticles and small agglomerates of nanoparticles are found on the alumina surface. It is interesting to notice that the agglomerates size is considerably smaller than for the as received Co_3O_4 ones. These small agglomerates are distributed randomly on the alumina microparticle instead of fully covering the surface of the microparticle. In addition, the observation of free space at the alumina surface could indicate a lack of available surface sites to host nanoparticles, which ever those sites can be. The dry dispersion procedure allows obtaining different hierarchical structures from nearly dispersed individual nanoparticles anchored on microparticles to isolated microparticles immersed in a nanoparticle matrix. Moreover, a control of the agglomeration state of the nanoparticles occurs by adjusting the amount of dispersed nanoparticles in the composite. As the amount of nanoparticles increases, small agglomerates start being formed in addition to the

dispersed nanoparticles. Similar behavior is observed for the different micro and nanoparticles used to carry out the nanodispersion process.

At this point it is necessary to establish statistical techniques that could evaluate the effectiveness of the dry dispersion procedure as well as to evaluate the control of the hierarchical structure. We observed a quite interesting and unusual behavior of the powder composites: meanwhile the used microparticles are white in color and the nanoparticles are black, the composites having low nanoparticles content acquired an unexpected brown color that change to grey as the amount of nanoparticles increased.

The nanoparticles under study have low diffuse reflectance in the UV–vis. However support microparticles are non-absorbent in the UV–vis range, which provides a high diffuse reflectance, Fig. 2a. Hence, a reduction of the reflectivity is expected for the composite powders. Fig. 2b shows the evolution of the reflectance at 400 nm for the different powder composites as a function of the nanoparticle amount. Low contents of nanoparticles (below 10 wt% in the case of Co_3O_4) drastically reduce the reflectance of the powder composite, while further increasing of the nanoparticles amount produce lower reduction of the reflectivity. The reflectance behavior of all the studied composites as a function of the nanoparticle amount presents similar non-linear behavior. This non-linear dependence of the diffuse reflectance reflects the effectiveness of the nanodispersion procedure. The amount of nanoparticles, <10 wt%, produces an effective covering of the microparticle surface. The nanoparticles form a layer covering effectively on the high reflectance microparticle surface, then reducing the diffuse reflectance of the powder composite. When the proportion of nanoparticles increased over this value, small agglomerates of nanoparticles are formed at the surface. The surface covering is then only slightly increased, and therefore the decrease of the reflectance is small with the addition of nanoparticles. These differences in the coverage degree of the surface by the nanoparticles produce the non-linear dependence and define the two different slopes of the absorbance as a function of the Co_3O_4 content. The maximum change of the reflectance slope, located at $\sim$10 wt% of nanoparticles, represents the nanodispersion limit and corresponds to the quantity above which large agglomerates are formed on the microparticle surface. Therefore, UV–vis diffuse reflectance provides relevant information of the nanodispersion degree in a fast and simple way.

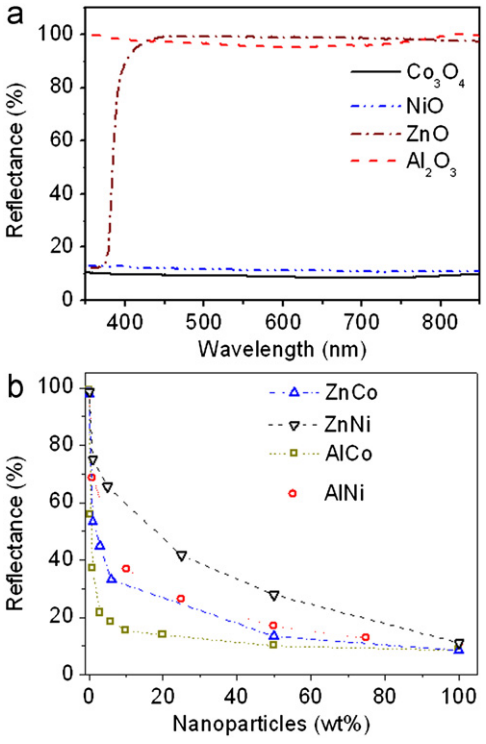

Fig. 2. (a) Reflectance of Al_2O_3, ZnO, Co_3O_4, NiO and (b) Reflectance of the sample versus nanoparticles proportion in the mixture.

Fig. 3 shows the net charge of the composites as well as the one of the as-received powders. A nonlinear variation of the net electrostatic charge of the composites is observed for mixtures of as-received powders having different charge polarity, Fig. 3a, and the same charge polarity, Fig. 3b. The addition of NiO or Co_3O_4 (positive charge) to the microparticles (Al_2O_3 positive and ZnO negative) to form the composites produce different values of the measured net charge. By the principle of linear superposition of the charge, the net charge of the dry powder composite obtained, Q_c, should follow the linear equation:

$$Q_c = (1-X)Q_M + XQ_N \quad (1)$$

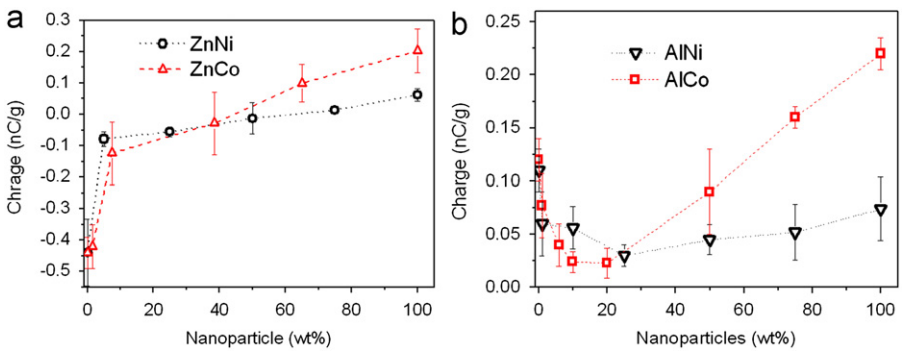

Fig. 3. Net electrostatic charge of powder composites: (a) ZnCoX and ZnNiX and (b) AlCoX and AlNiX.

where Q_M and Q_N are the net charge of the microparticles and nanoparticles respectively, and X is the normalized percentage in weight of the nanoparticles. As expected, when the particles have different polarity of the net charge, ZnO (negative) and Co_3O_4 and NiO nanoparticles (both positive), there is a compensation of the charge when the maximum dispersion is obtained, Fig. 3a. It is worth mentioning that there is a strong compensation of the charge for the smallest amount of nanoparticles in the mixture, < 10 wt%. Once this point is reached, the changes of the net charge in the composites vary slowly with the nanoparticles amount. On the other hand, when microparticles and nanoparticles have the same net charge polarity, Al_2O_3 (positive) and Co_3O_4, NiO (positive), Fig. 3b, a partial compensation of the electrostatic charge appeared for a particular content of nanoparticles. In both cases the non-linear behavior resembles the previously observed non-linear dependence of the diffuse reflectance for the dry formed powder composites.

Fig. 4 shows infrared spectroscopy of the different as-received powders to analyze possible surface differences responsible for the observed behavior of the charge of powder composites. Infrared spectroscopy is an optical technique suitable for the study of the material surfaces and which can provide information about the chemical structure of the analyzed material by the nature of bonds vibration. Traces of polymers or organic material were not identified and the only differences were observed at the wavenumber region of 3200–3800 cm^{-1}, related to surface adsorbed OH groups. Since the energy of vibration of these groups change as a function of the nature of the adsorbing place at the particle surface, the variation of the OH group for all samples points out that the different samples have different types of OH groups. Due to this different nature, the OH groups can provide different charge to the particles surface [15]. Due to the earlier mentioned nature, the OH groups of the different particles can interact between them. This interaction takes place due to an acid–base electrochemical reaction which compensates the electrostatic charge provided by the hydroxyls groups at the dissimilar surfaces [16]. Thus, the better the dispersion, the higher the net charge compensation.

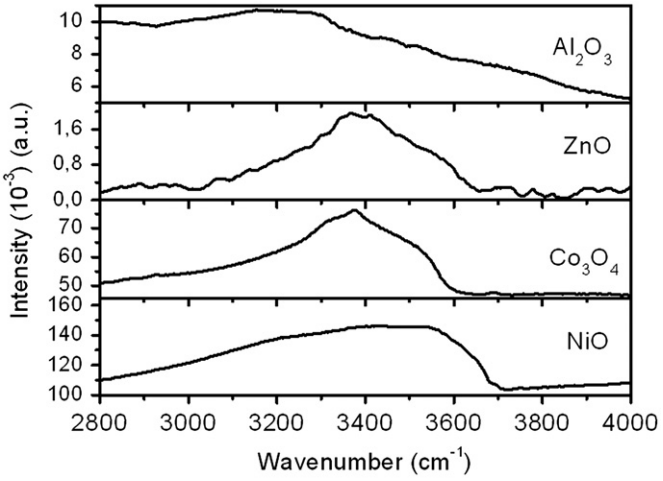

Fig. 4. Infrared Spectroscpy (ATR) of Al_2O_3, ZnO, Co_3O_4, NiO.

During tribo-charge experiment, the microparticles acquire electrostatic charge by friction with the glass tube. ZnO microparticles also showed a change of polarity that could be attributed to presence of different morphologies that the powder presents, i.e. needle shaped ZnO grows in the wurzite structure along the (001) direction alternating zinc and oxygen layers which allow the presence of hydroxyl groups associated to surface defects [19].

The tribo-charge is also measured as a function of the nanoparticles amount in the powder composites, Fig. 5. For better comparison purposes the average agglomerate size after tribo-charge measurement is also included. There is a clear correlation between tribo-charge and agglomeration size of the powder composites. Both the tribo-charge and the agglomerate size reach maximum values for the same nanoparticles content in the powder composite. This nanoparticle amount corresponds to the one which possesses the highest net electrostatic charge compensation and then to the best dispersion of the nanoparticles. In spite of the non-linear dependences observed the composites showed surprising changes in their agglomeration state depending on the nanoparticles content. For simplicity, Fig. 6 shows optical micrographs of the representative samples AlCo1 and AlCo50. It can be seen that the proportion of the nanoparticles changes drastically the agglomerate size. The large agglomerates observed on AlCo1 seem to be highly packaged. By the contrary, higher amount of nanoparticles produced smaller powder composites agglomerates, showing voids and therefore resulting in lower packaging state. The observed effects resulted from the appearance of nanoparticles hierarchically ordered at the surface of the microparticles. The nanoparticle presence at the microparticle surface modified the composite formation mechanism during the electrostatic charge accumulation. Fig. 7 shows a schematic model of the composite structure related to the nanodispersion state in the powder composite. The nanodispersion of the nanoparticles at the microparticle surface enhanced their surface roughness and provides a better adhesion of microparticles. The process can be easily described as a "zip". The nanoparticles promote the adhesion between microparticles and in addition the composite packaging. The agglomerate size correlated with the tribo-charge indicating that electrostatic accumulation is proportional to the total surface of the composite agglomerate.

The increase of nanoparticles amount in the powder composites over 10 wt% produce a higher number of nanoparticles agglomerates. The contact between microparticles is then reduced and the composite present packaging defects. The size of the composites agglomerates is reduced, reducing also the tribo-charge.

This methodology describes a simple way for the formation of powder composites having different nanoparticle/

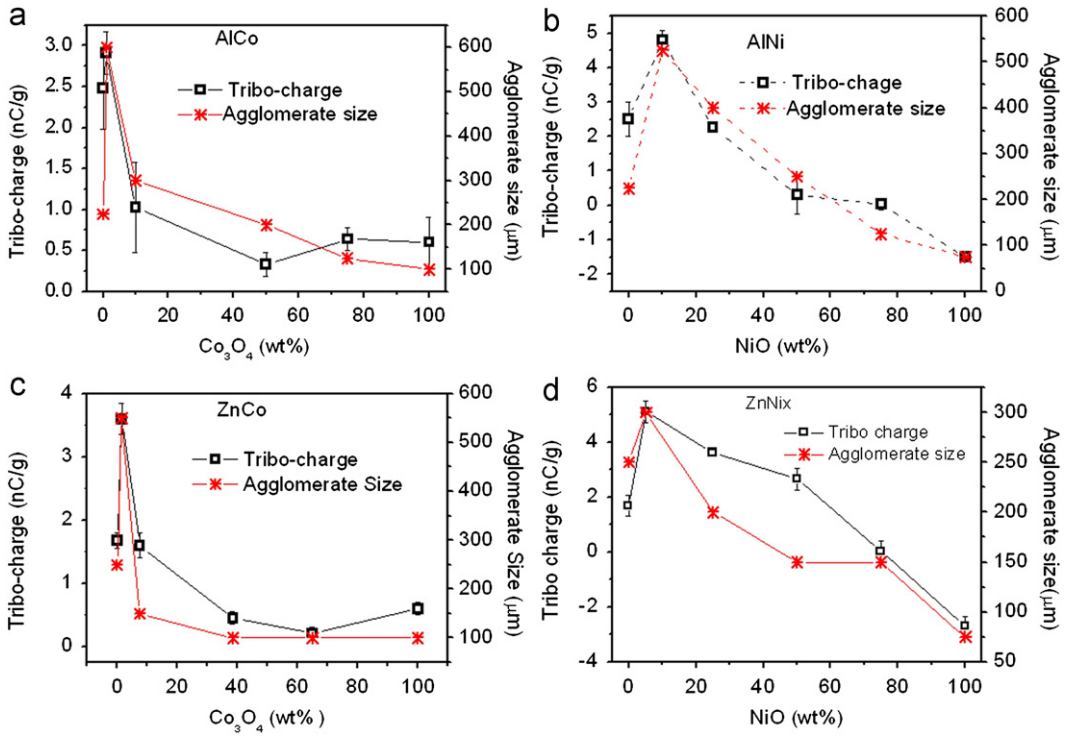

Fig. 5. Tribo-charge and agglomerate size of the powder composites as a function of the nanoparticle amount: (a) AlCoX; (b) AlNiX; (c) ZnCoX and (d) ZnNiX.

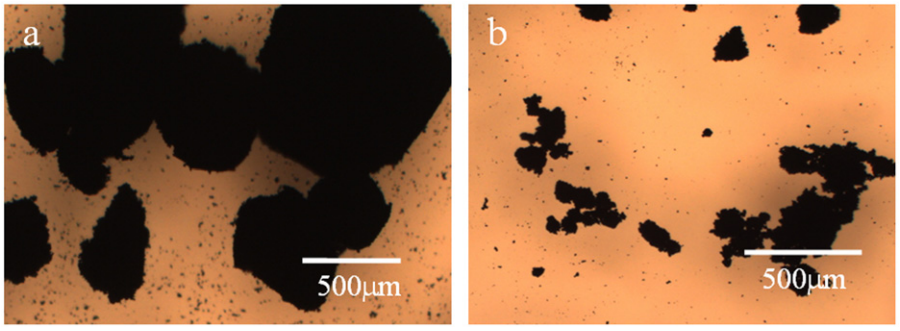

Fig. 6. Representative micrographs obtained by Light Reflected Optical Microscopy of AlCo1 (a) and AlCo50 (b) powder composites.

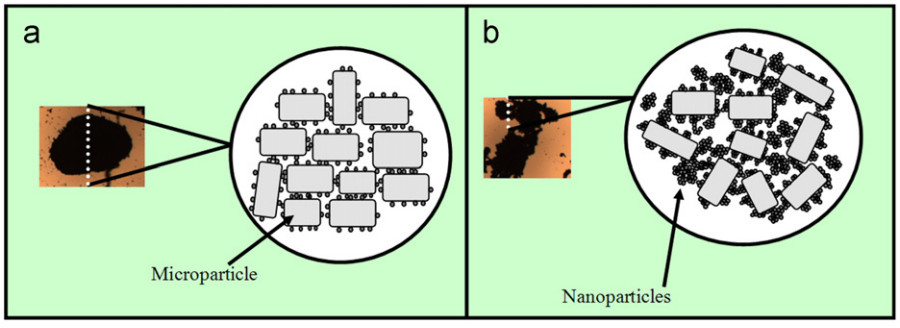

Fig. 7. Modeling of the powder composites particles distribution for different proportions of nanoparticles in the mixture: (a) nanodispersion at 1 wt% and (b) nanodispersion and small agglomerated at >10 wt%.

microparticle distribution. The composites are formed by using the dry dispersion procedure. One of the advantages of this procedure is the simplicity. Moreover, methodologies to evaluate the dispersion efficiency by using UV visible spectroscopy and electrostatic measurements contributed to the understanding of the formation processes. The powder composites here described open opportunities for the materials development. Powder composites could

serve as vector for disperse nanoparticles incorporation in different matrixes, i.e., polymeric or ceramic or metallic ones. The powder composites could serve as agglomerates to conform composite materials in different applications, as coating for electrodes or fillers for nanomaterial processing.

4. Conclusions

The formation mechanism of nanoparticles/microparticle hierarchical composites has been described. The dispersion of different type of nanoparticles over microparticles, as support or substrate, has been afforded by a soft mechanical and solvent-less procedure. The powder composite showed different hierarchical order as a function of the nanoparticle amount. Low nanoparticle amounts, < 10 wt%, produced a dispersion of nanoparticles that remained anchored at the microparticle surface. Higher amount of nanoparticles produce the appearance of agglomerates of nanoparticles or even a matrix of nanoparticles including dispersed microparticles.

The dispersion degree can be evaluated by using diffuse reflectance measurements. A non-linear dependence of the diffuse reflectance as a function of the nanoparticles amount is observed. At this point also nonlinear compensation of the net electrostatic charge appeared due to the consumption of the surface OH groups mediated by a redox reaction. This interaction provides the anchoring mechanism of the nanoparticles onto the microparticles. The dispersed and anchored nanoparticles provide a roughness increase of the microparticles surface that is responsible for a formation of nanoparticle/microparticle composite powders following a "zip" effect in which tribo-charge maximized. This effect enhanced packaging of composites and allows reaching a maximum size of the powder composites.

Acknowledgment

This work has been financially supported by Project MAT2010-21088-C03-01.

References

[1] J. Jiang, G. Oberdörster, Characterization of size, surface charge, and agglomeration state of nanoparticle dispersions for toxicological studies, Journal of Nanoparticle Research 11 (2009) 77–89.
[2] L.Lu Chen, J. Li, Z. Yu, W. Kong, H. Zhu, Journal of Power Sources 196 (2011) 3178–3185.
[3] J. Yu, Y. Su, B. Cheng, Advanced Functional Materials 17 (2007) 1984–1990.
[4] D. Genovese, M. Montalti, L. Prodi, E. Rampazzo, N. Zaccheroni, K. Altenhöner, F. May, J. Mattay, Chemical Communications 47 (2011) 10975–10977.
[5] M.S. Martín-González, J.F. Fernández, F. Rubio-Marcos, I. Lorite, J.L. Costa-Krämer, A. Quesada, M.A. Bañares, J.L.G. Fierro, Insights into the room temperature magnetism of ZnO/Co_3O_4 mixtures, Journal of Applied Physics (2008) 083905.
[6] F. Rubio-Marcos, C.V. Manzano, J.J. Reinosa, I. Lorite, J.J. Romero, J.F. Fernández, M.S. Martín-González, Modification of optical properties in ZnO particles by surface deposition and anchoring of NiO nanoparticles, Journal of Alloys and Compounds 509 (2011) 2891–2896.
[7] M. Haruta, Size- and support-dependency in the catalysis of gold, Catalysis Today 36 (1997) 153.
[8] R.P. Andres, J.D. Bielefeld, J.I. Henderson, D.B. Janes, V.R. Kolagunta, C.P. Kubiak, W.J. Mahoney, R.G. Osifchin, Self-assembly of a two-dimensional superlattice of molecularly linked metal clusters, Science 273 (1996) 1690.
[9] R.G. Freeman, K.C. Grabar, K.J. Allison, R.M. Bright, J.A. Davis, A.P. Guthrie, M.B. Hommer, M.A. Jackson, P.C. Smith, D.G. Walter, M.J. Natan, Science 267 (1995) 1629.
[10] S.L. Westcott, S.J. Oldenburg, T. Lee, N.J. Halas, Langmuir 14 (1998) 5396–5401.
[11] Y. Luoa, J. Zhub, Y. Mab, H. Zhang, International Journal of Pharmaceutics (2008) 35816–35822.
[12] J.A. Hersey, Powder Technology 11 (1975) 41–44.
[13] M. Murtomaa, E. Laine, Journal of Electrostatics 48 (2000) 155162.
[14] J. Goniakowski, C. Noguera, Surface Science 330 (1995) 337–349.
[15] I. Lorite, M.S. Martín-González, J.J. Romero, M.A. García, J.L.G. Fierro, J.F. Fernández, Ceramics International 38 (2) (2012) 1427–1434.
[16] M.S. Martin-González, M.A. García, I. Lorite, J.L. Costa-Krämer, F. Rubio-Marcos, N. Carmona, J.F. Fernández, Journal of the Electrochemical Society 157 (3) (2010) E31–E35.
[17] J.F. Fernandez, I. Lorite, F. Rubio-Marcos, J.J. Romero, M.A. Garcia, A. Quesada, M.S. Martin-Gonzalez, J.L. Costa-Kramer, Patent no. WO2010010220-A1, 2010.
[18] I. Lorite, J.J. Romero, J.F. Fernández, Factors affecting the electrostatic charge of ceramic powders, Boletin de la Sociedad Espanola de Ceramica y Vidrio 50 (2) (2011) 73–78.
[19] H. Noei, H. Qiu, Y. Wang, E. Löer, C. Wöll, M. Muhler, Physical Chemistry Chemical Physics 10 (2008) 7092–7097.